Iraqi Journal of Oil & Gas Research

Journal homepage: https://ijogr.uotechnology.edu.iq

Variation of Total Stresses During Field Operation Using Finite Element Technique, Zubair Oil Field.

Ali Khaleel Faraj[1,] , Ameen Kareem Salih[1], Hassan Abdul Hadi Abdul Hussein[2] and Ali Nahi Abed Al-Hasnawi[3]*

[1] Oil and Gas Engineering Department, University of Technology-Iraq, Baghdad-Iraq
[2] Petroleum Engineering Department, College of Engineering, University of Baghdad, Iraq
[3] Drilling Branch, Petroleum Engineer, Islamic Azad University, Tehran - Iran

Article information

Article history:
Received: February, 22, 2023
Accepted: March, 30, 2023
Available online: April, 08, 2023

Keywords:
3D geomechanical model;
Finite element method;
Total stress;
Couple model;
1D earth model

Corresponding Author:
Ali Khaleel Faraj
150103@uotechnology.edu.iq

Abstract

The Zubair oil field is predominantly plagued by geomechanical issues, which can result in significant non-productive time. The aim of this study is to present a reservoir model and a geomechanical model utilizing the finite element method. The intriguing data consisting of logs, calibration data, drilling reports, and mud reports were utilized to construct one-dimensional models (1D) for each well using Techlog 2015 software. Furthermore, the 3D geomechanical model was built utilizing Petrel 2017 software, while the finite element technique was implemented using the CMG 2018 program to predict the total stress states during production or injection operations in the field over a span of 10 years.The analysis results of all mechanical rock properties in the 3D geomechanical model revealed that Shuaiba and Al-Hammar domes were insufficient for maintaining stable wells, particularly in the Tanuma formation. However, the Mishrif formation displayed higher stability despite production. Furthermore, the 3D finite element model exhibited that the total horizontal stress decreased during production and increased in injection wells. This variation would result in an increase in the effective horizontal stress during production and a decrease in injection wells. Moreover, the effective vertical stress increased during production and decreased during injection wells. Based on these outcomes, it can be concluded that production could trigger an increase in the differential stress leading to rock shear failure, whereas in injection cases, pore pressure increased, and this caused tensile failure.

DOI: http://doi.org/10.55699/ijogr.2023.0301.1036, Oil and Gas Engineering Department, University of Technology-Iraq

1. Introduction

The geomechanical study is a field of science that focuses on the collection and analysis of data related to the geological and mechanical properties of rocks. This involves examining how rocks may deform or fail as a result of production or injection processes [1]. One of the major challenges in geomechanics is wellbore instability during drilling operations, which can result in significant non-production time (NPT) and financial losses, [2].

The non-productive time (NPT) was the major problem that can have happened from wellbore instability will be caused high costs during the drilling operation. To minimize this cost it's necessary to understand and calculate the stresses that caused the wellbore instability. Any change in the stresses about the wellbore will be caused instability and trouble [3]. The change in the formation pressure during the production or injection leads to a change in two important stresses (total and effective) which can cause different geomechanical troubles [4]. Geomechanical troubles can be subsidence problems which may be like porous compaction, pipe harm, well casing smash, and tensile or failure of the borehole [5]. Shear failure (break out) Means the collapse of the well wall due to insufficient drilling fluids that support the wall and thus makes the stresses around the wall exceed the pressure obtained through the drilling process. Tensile failure (break down) means that the pressure caused by drilling mud is much higher than the pore pressure or stress around the wellbore which can lead to formation fracture and mud losses [6].

The determination of stress distribution requires the utilization of various models. Firstly, a 1D mechanical earth model, which includes pore pressure calculations, rock mechanical properties, and initial in-situ stresses, is used to understand the state of stresses surrounding the wellbore [7]. Secondly, a 3D geological model is utilized to distribute rock mechanical properties and pore pressure for the entire field. Lastly, a 3D finite element model is used to calculate the stress distribution during pore pressure changes. This research incorporates a coupling of the reservoir and geomechanical models to predict the state of stress during production or injection for a certain period.

1.1. Area of Study

The Zubair oil field, situated approximately 20 kilometers southwest of Basra as depicted in Figure-2, is one of the largest oil fields in Iraq. Its discovery dates back to 1949, with construction commencing in 1951. According to Iraq's tectonic zones, the Zubair oil field lies in the sagging pelvis of the Mesopotamian zone, which forms part of the Arabian plate's quasi-platform foreland, [8]. The Euphrates subzone, Tigris subzone, and Zubair subzone are the three subzones of the Mesopotamian zone. The study region is located within the Zubair subzone, which was given the designation Basrah zone in 1979 by an Iraqi-Soviet team. The Alpine orogenic motions (basement faults and salt formations) make the Zubair subzone unstable. These elements are to blame for the formation of subsurface anticline structures in Iraq's southern regions [9].

The geological stratigraphic column of the Zubair oil field, as shown in Figure-1, is characterized by a thick succession of Cretaceous carbonates that contain substantial amounts of hydrocarbon accumulations. The Zubair and Rumaila oil fields, in general, and the Mishrif and Zubair formations, in particular, are the most significant producers of hydrocarbons in the Iraqi field. The Mishrif and Zubair formations originate from the Chiagara in the upper Jurassic and Sargelu in the middle Jurassic, which serve as the parent rocks, [10].

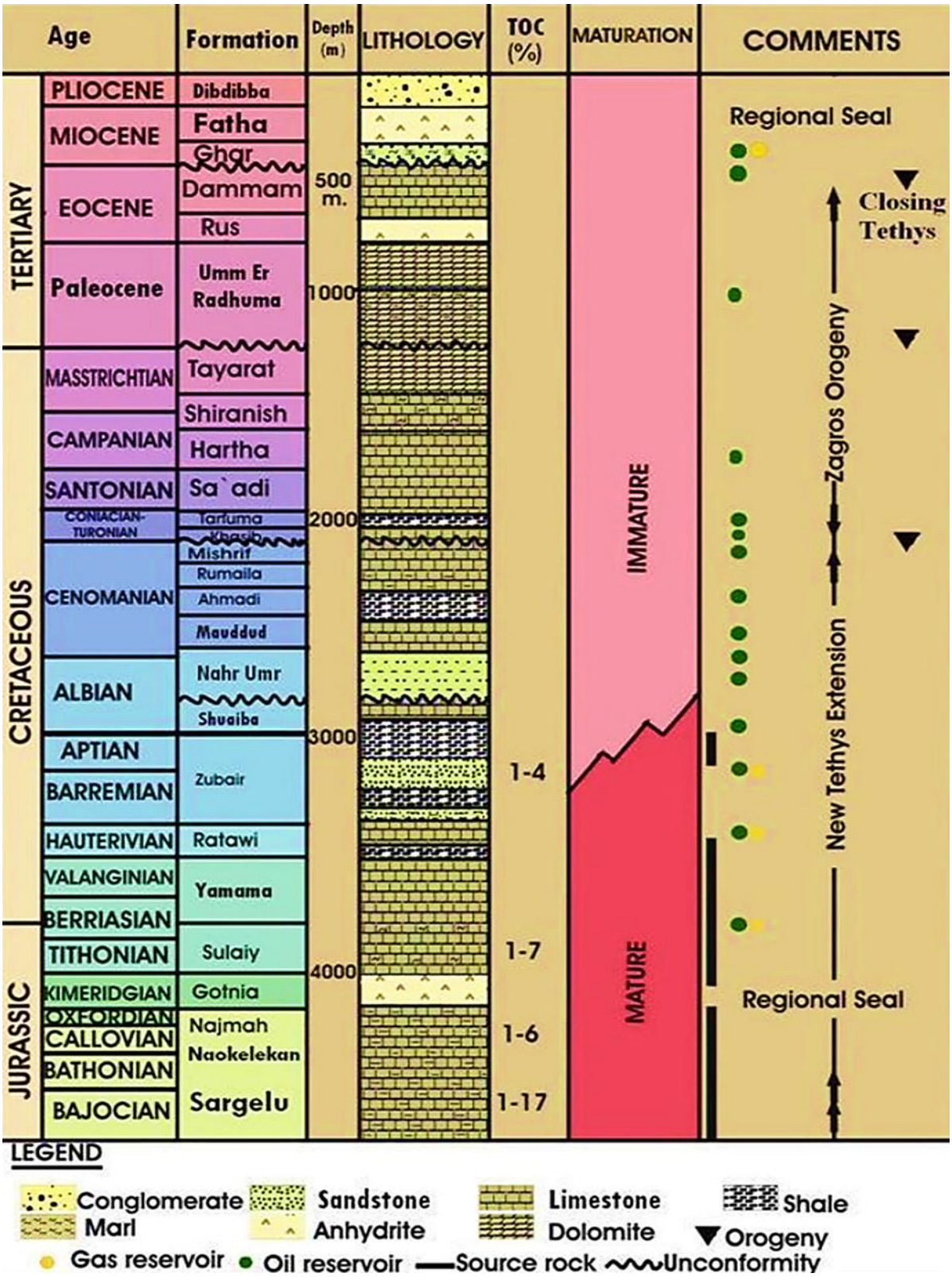

Figure 1: The geological structure of the Zubair oil field, [11].

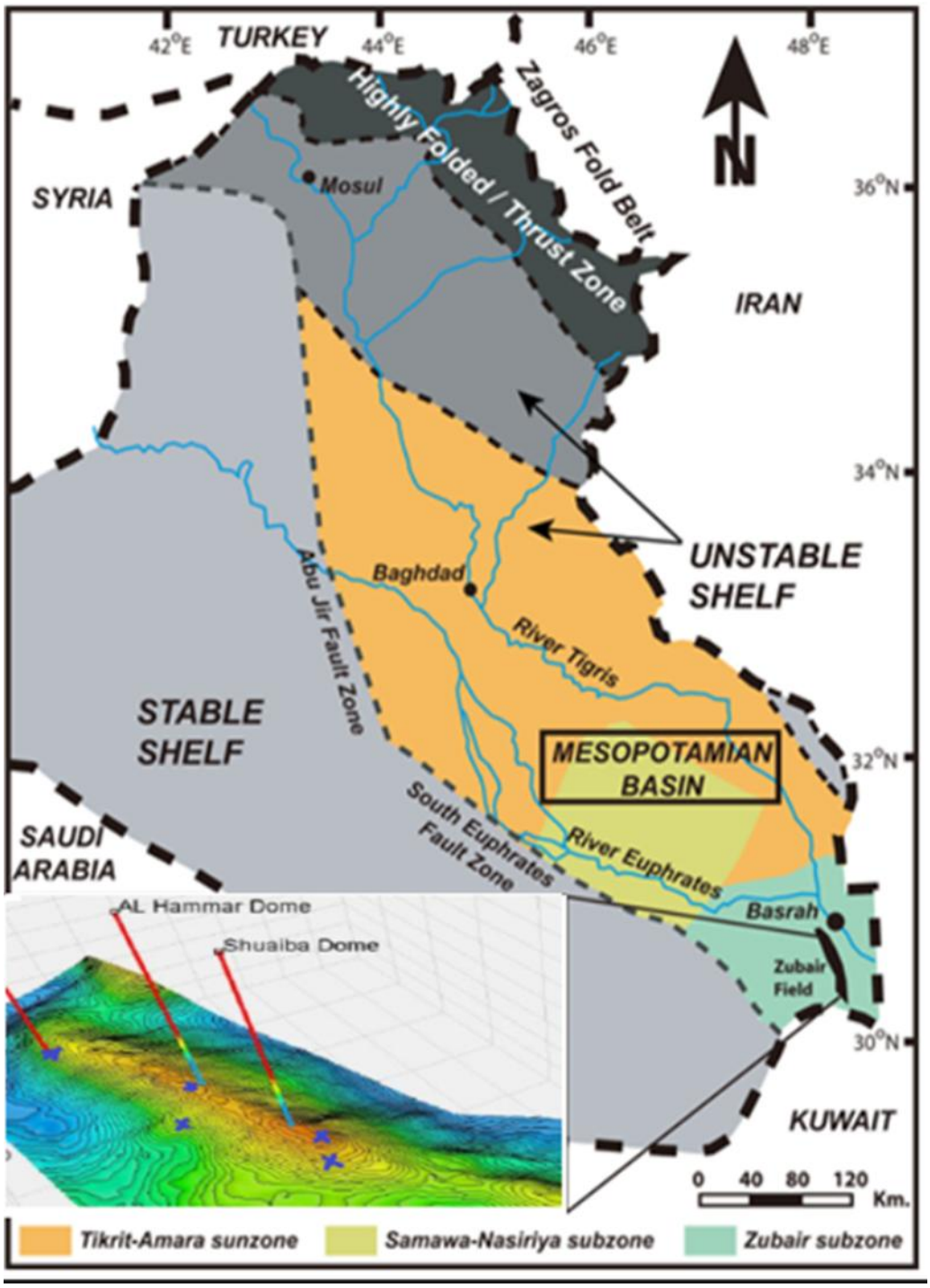

Figure 2: The Mesopotamian Basin's geology of Zubair Field with a map of the locations of the investigated wells, [12,13,14].

2. Methodology

The creation of a geomechanical model presents a common challenge in the form of requiring a diverse range of data sources [15]. For the north portion of the Zubair oil field, data was collected from various production wells (ZA-2, ZA-3, and ZA-44) and injection wells (ZA-24 and ZA-36) that cover two domes - Shuaiba and Al-Hamar. Due to drilling complexities, such as wellbore instability and drilling mud loss, Section 12.25 was selected for drilling the wells. This section allowed for the penetration of six layers: Sadi, Tanuma, Khasib, Mishrif, Rumulla, and Ahmadi.

The available data consisted of mini-frac, core test, and various logs, including gamma-ray, caliper, bit size, density, and sound logs (shear and compression). The rock mechanical properties were calibrated through Brazilin and triaxial tests. In addition, pore pressure results were calibrated using formation pressure point data. Horizontal stress results were matched using fracture tests.

2.1. 1D Model

The 1D model, illustrated in Figure-3, comprises various elements such as vertical stress, mechanical shale flag, formation pressure, elastic and strength rock properties. Based on the available data, the model then calculates the horizontal stresses. The vertical stress, also known as overburden stress, is determined using "Equation (1)," where in the density log readily provides the overburden stress, [16]. Several approaches can be used to determine bulk density, but the extrapolated density approach provides the most accurate results. By correcting any existing grammar errors, we ensure the accuracy of our findings, [17].

$$Sv = \int_0^z p\,(z)\;\; g\; dz \qquad (1)$$

Where Sv is vertical stress, ρ is the bulk density and z was total depth.

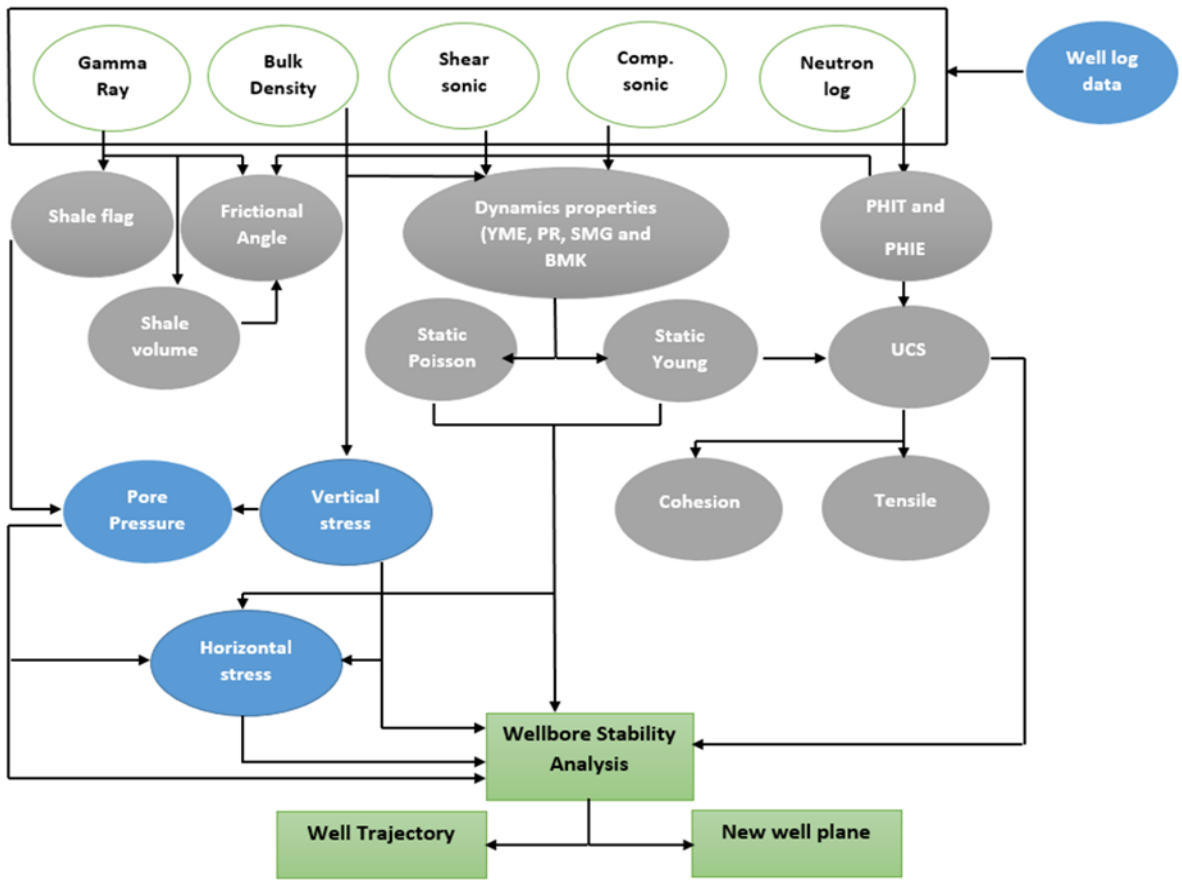

Figure 3: Workflow for 1D model.

Unlike other procedures, the bowers method was used to calculate pore pressure, as stated in "Eq. (2)", which was reliant on the pressure generated by both the compaction and fluid expansion mechanisms [18]. Bowers' approach yields significantly superior forecast results compared to the Eaton's technique, [19].

$$PE = PO - \propto .PP \quad (2)$$

Where: PE is the effective stress, PO is the overburden pressure, PP is pore pressure, and α is the effective stress coefficient which is less than 1.

Young's modulus and Poisson ratio are elastic rock properties, whereas rock strength properties are cohesion, unconfined compressive strength, frictional angle, and tensile strength. Because static characteristics can't be derived directly from log data, dynamic properties should first be determined using density, shear, and compression velocity logs. Dynamic shear modulus (G) and dynamic bulk modulus (K) were calculated using "Equation. (3)" and "Equation. (4)", respectively, while dynamic young's modulus and Poisson ratio were calculated using "Equation. (5)" and "Equation. (6)" [20].

$$Gdyn = 13474.45 \frac{\rho_b}{(\Delta t\ shear)^2} \quad (3)$$

$$Kdyn = 13474.45 \frac{\rho b}{(\Delta t\ shear)^2} - \frac{4}{3} Gdyn \quad (4)$$

$$Edyn = \frac{9\ Gdyn \times Kdyn}{Gdyn + 3\ Kdyn} \quad (5)$$

$$Vdyn = \frac{3\ Kdyn - 2\ Gdyn}{6\ Kdyn + 2\ Gdyn} \quad (6)$$

Where Gdyn is dynamic shear modulus Kdyn dynamic bulk modulus, ρb is bulk density in gm/cm3 and t shear is sonic shear velocity while Edyn is dynamic young's modulus and Vdyn is dynamic Poisson ratio.

2.2. 3D Geomechanical Model

Using the petrel 2017 software, a three-dimensional model 3D was created in this part. Petrel software was used to create a 3D geological model for six formations, including the Sadi, Tanuma, Khasib, Mishrif, Rumaila, and Ahmadi formations, as indicated above. The first data required for this model was wellhead and well tops, which contained all wells and layer information. The second data was a contour map or a structural contour map, which contained contour elevation, and the final data was well logs. These data are the main results of a 1D mechanical earth model, which contains rock mechanical properties such as Poisson ratio, internal frictional angle, Young's modulus, unconfined compressive strength, tensile strength, and pore pressurization. The workflow chart in Figure-4 below depicts all the steps involved in creating a 3D geomechanical model.

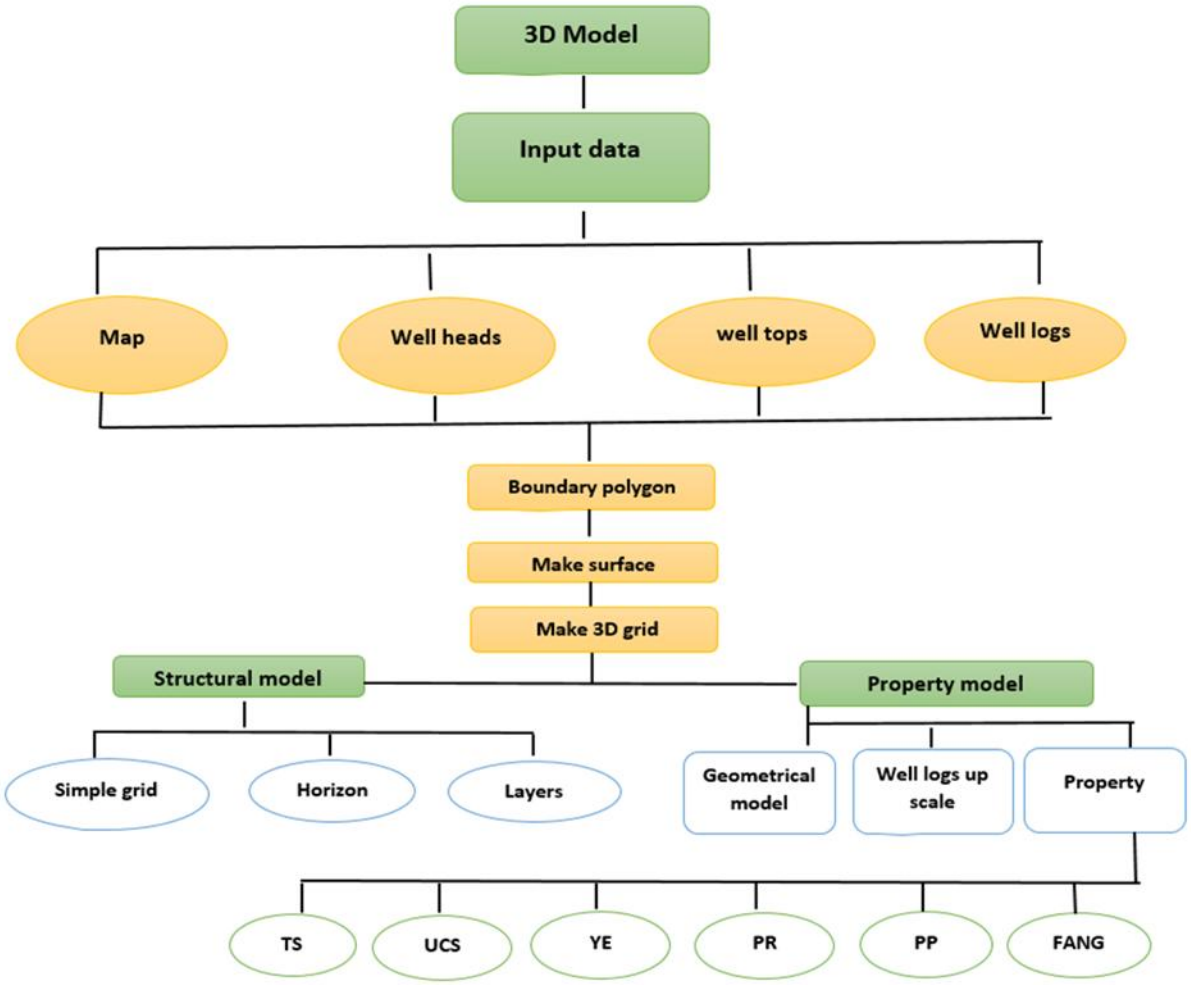

Figure 4: Workflow diagram for a 3D model.

2.3. 3D Finite Element Model

The finite element analysis was performed using the computer modeling company (CMG) 2018 software to distribute and measure the bottom stresses in all directions as indicated in "Eq. (7)", "Eq. (8)" and "Eq. (9)". Typically, reservoir models (injection or production) do not account for changes in reservoir stress, so it is necessary to couple these two models. The IMEX simulator was one of three simulators that the company demonstrated for the black oil model, and it was able to couple the geomechanical model and the fluid model. The CMG program uses the findings of a 3D geological model created with Petrel software as input data, which includes rock mechanical characteristics and pore pressure after distribution in each grid.

$$\sigma x = \frac{E}{(1+V)(1-2V)}[\varepsilon x(1-V) + V\varepsilon y + V\varepsilon z] \quad (7)$$

$$\sigma y = \frac{E}{(1+V)(1-2V)}[V\varepsilon x + (1-V)\varepsilon y + \varepsilon z] \quad (8)$$

$$\sigma z = \frac{E}{(1+V)(1-2V)}[\varepsilon x + \varepsilon y + (1-2V)\varepsilon z] \quad (9)$$

Where σx, σy, and σz are normal stress, E is young's modulus, v is a Poisson ratio, and εx, εy, and εz are the normal strain.

3. Results and Discussion

3.1. Mechanical Earth Model

The findings of the one-dimensional mechanical earth model are depicted in Figure 5. The vertical stress was determined by employing the extrapolation method in the second track. Furthermore, the results of the pore pressure testing are also presented in the second track.

The static Young's modulus in the third track, evaluated using Modified Morales correlation (YME-STA-MMC), was dependent on total porosity and dynamic Young's modulus, as seen in the preceding tracks [20]. In the fourth track, the static Poisson ratio was frequently calculated using the dynamic Poisson ratio, which is prevalent in rock characteristics [21]. Unconfined compressive strength (UCS-YME) is predicted using static Young's modulus correlation in the fifth track, then tensile stress is calculated using UCS results in the sixth track, and the frictional angle is calculated using log tools (neutron, density, and gamma-ray) in the seventh track,

The first track also contains the horizontal stress (max and min) with vertical stress, normally the direction of max horizontal stress in vertical wells is perpendicular to the direction of min horizontal stress [22]. The min horizontal stress shows a good match with min-frac points data. From the stresses results were shown in this track and depending on Anderson (1951) classifies the faults regime for section 12.25" in Zubair field can prediction.

Calibration data is shown in black circles, as well as checks to ensure that the estimated mechanical parameters are valid. All of the mechanical properties are in good agreement with the calibration points. Pore pressure matched the formation pressure positions in the black circles pretty well. Due to the availability of our data, the results of making 1D for five wells are satisfactory.

3.2. 3D Geomechanical Results

3.2.1. Frictional Angle (FANG)

The frictional angle, which refers to soil quality and rock hardness [23], was the first property distribution. The results for Tanuma and Mishrif formations were shown in Figure-6. As can be observed, the frictional angle has a minimum value in the Tanuma formation and a maximum value in the Mishrif formation. Tanuma is said to be less stable than Mishrif. The best values were found in the Rumilla, Khasib, Ahmadi, and Sadi formations, with about 70% of the data having a high angle, which is favorable for borehole stability, according to the histogram data for this feature in all formations

3.2.2. Unconfined Compressive Strength

The Tanuma and Mishrif formations are shown in Figure-7. In this graph, nearly 84 percent of the UCS data distribution was between 500 and 4000 psi, which are low values that can cause wellbore instability. The Shuaiba and Al-Hammar domes were the focus of these minimal values. According to results, around 40% of the data had minimum values, while 60% of the data was considerably better. The finest UCS property distribution values were in Mishrif at around 80%, although there were the lowest values from the data between 4000 and 9000 psi.

3.2.3. Poisson ratio (σ)

In the geomechanical model, the values of the Poisson ratio are essential. It refers to the rock deformation that occurs during the drilling process. The 3D distribution of the Poisson ratio was shown in Figure-8, whereas Figure-9 was the outcome of this feature in the Tanuma and Mishrif formations. In the Tanuma formation, high values of Poisson ratio focus in the Shuaiba and Al-Hammar domes accounted for around 65 percent of the data, which is not ideal for wellbore stability. From the data, Mishrif formations provided the lowest Poisson ratio values of around 90%, which is usually the optimum for wellbore stability.

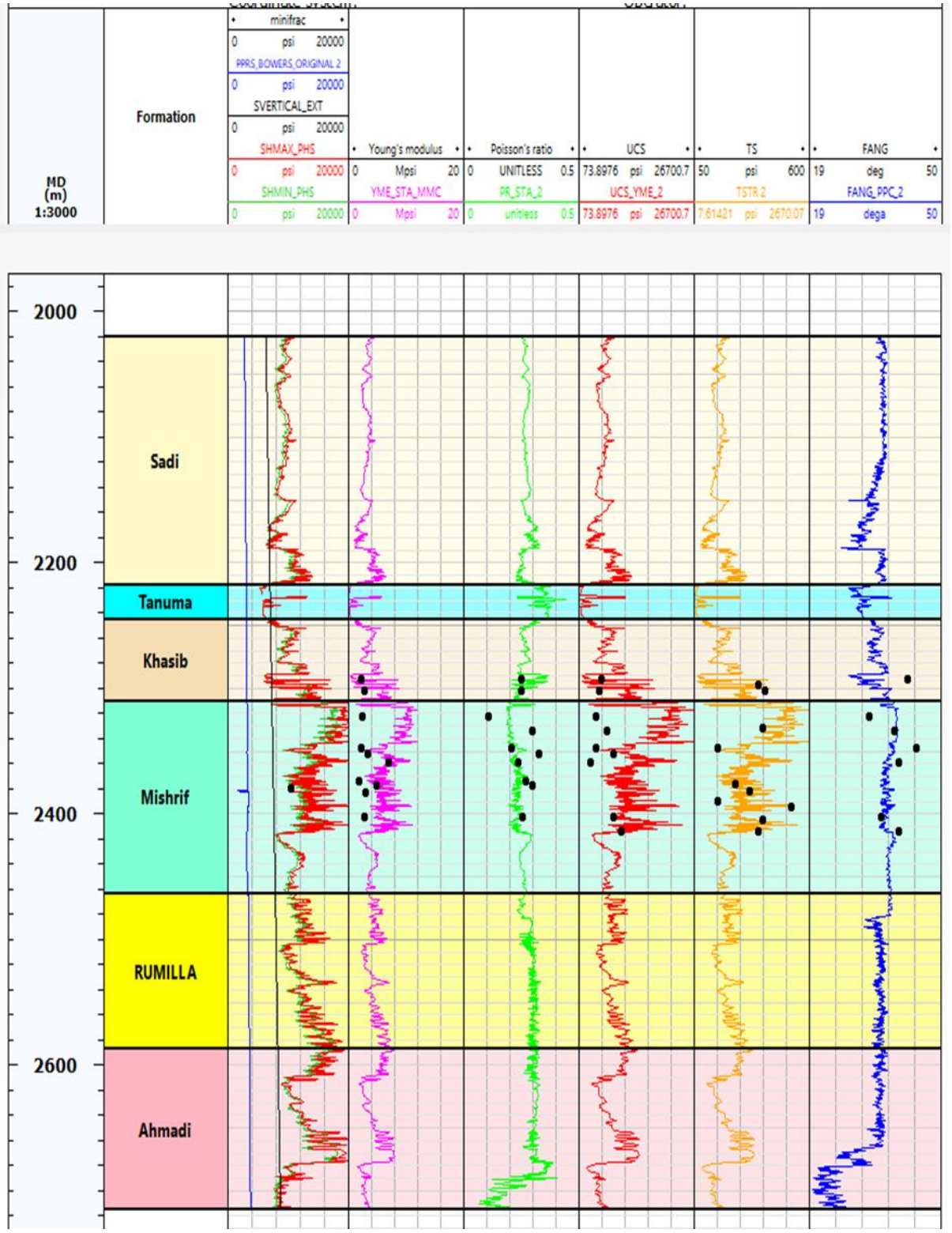

Figure 5: 1D mechanical earth model for ZA-24 well in Zubair oil field

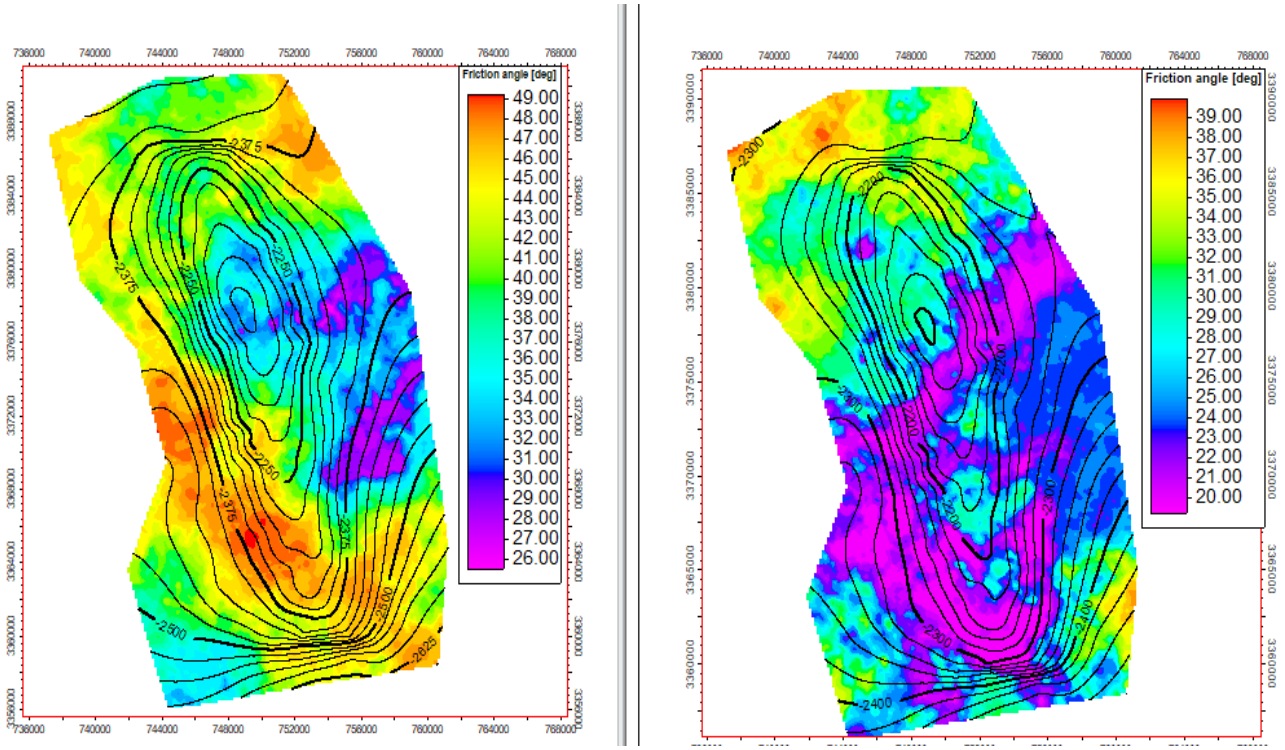

(a) **(b)**

Figure 6: Frictional angle distribution map for; (a) Mishrif formation and (b) Tanuma formation.

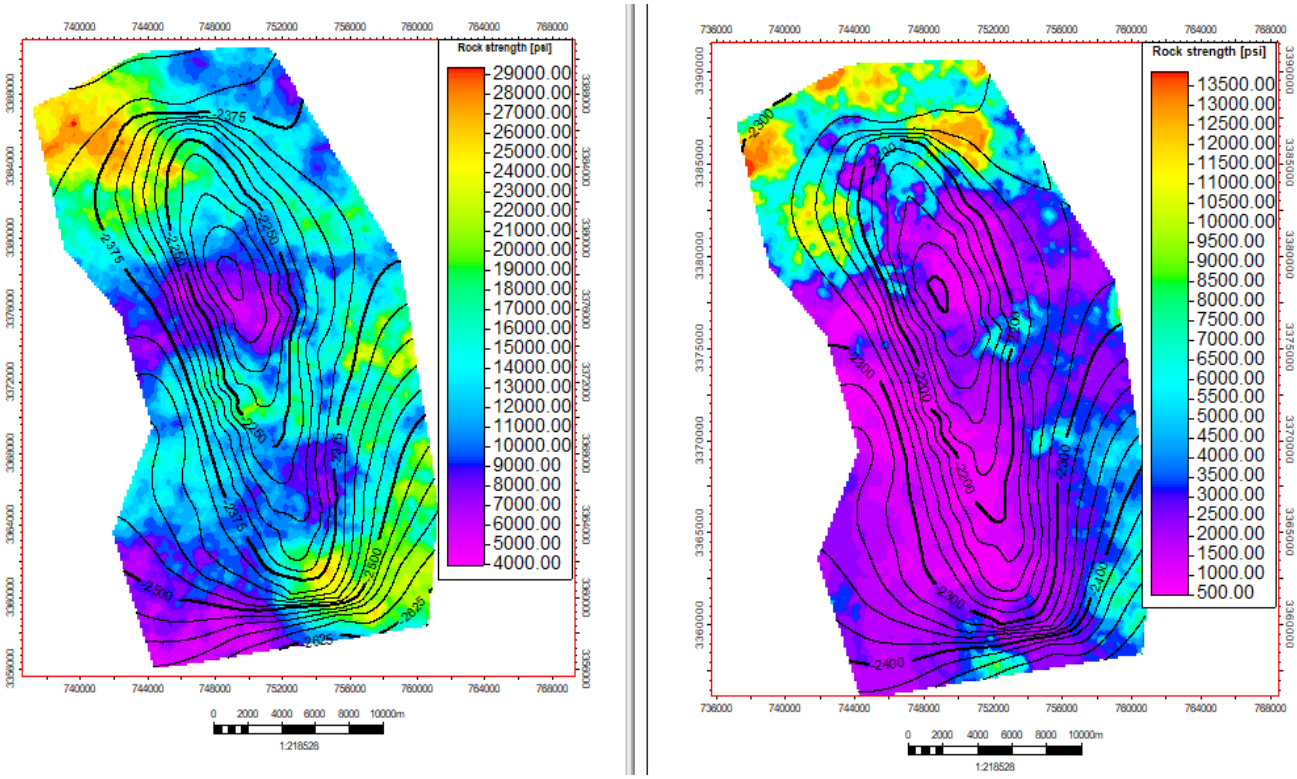

(a) **(b)**

Figure 7: Unconfined Compressive Strength distribution map for; (a) Mishrif formation and (b) Tanuma formation.

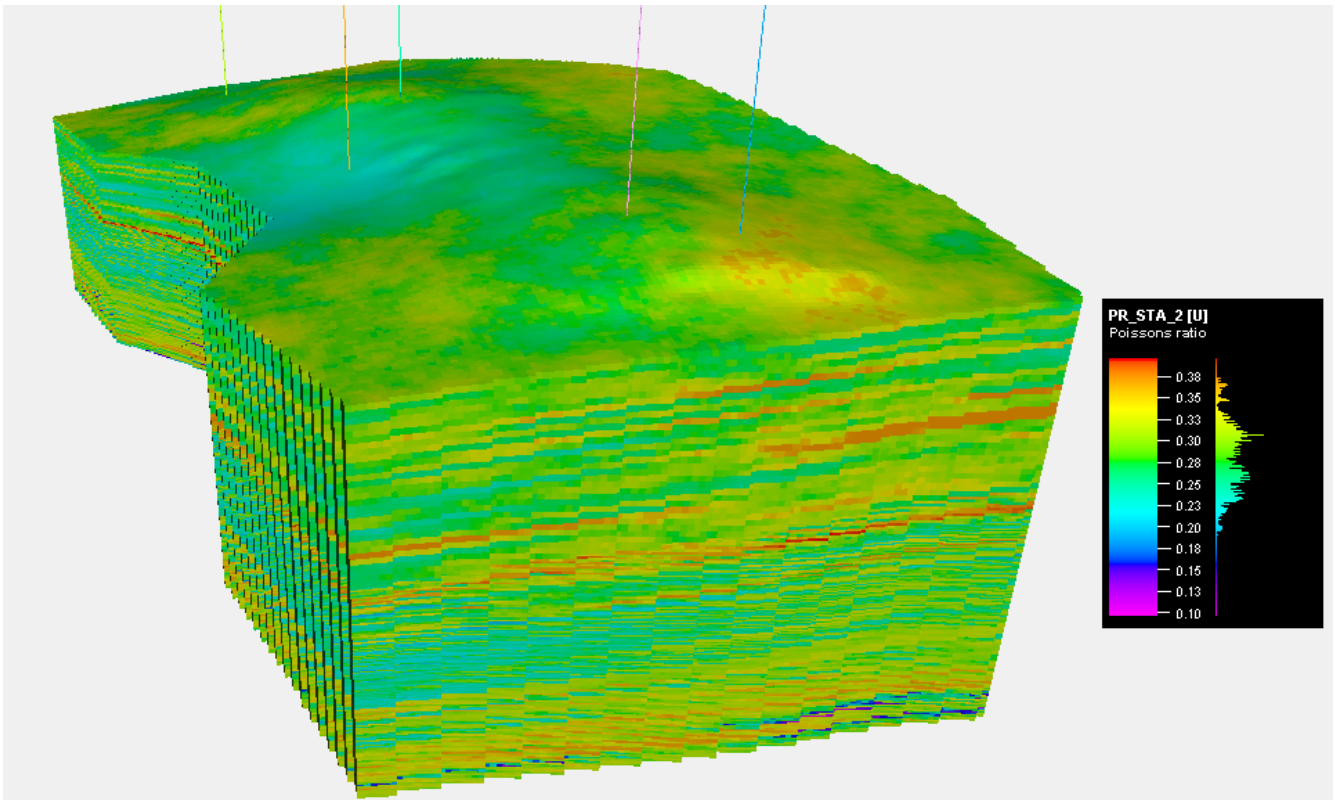

Figure 8: 3D distribution map for Poisson ratio.

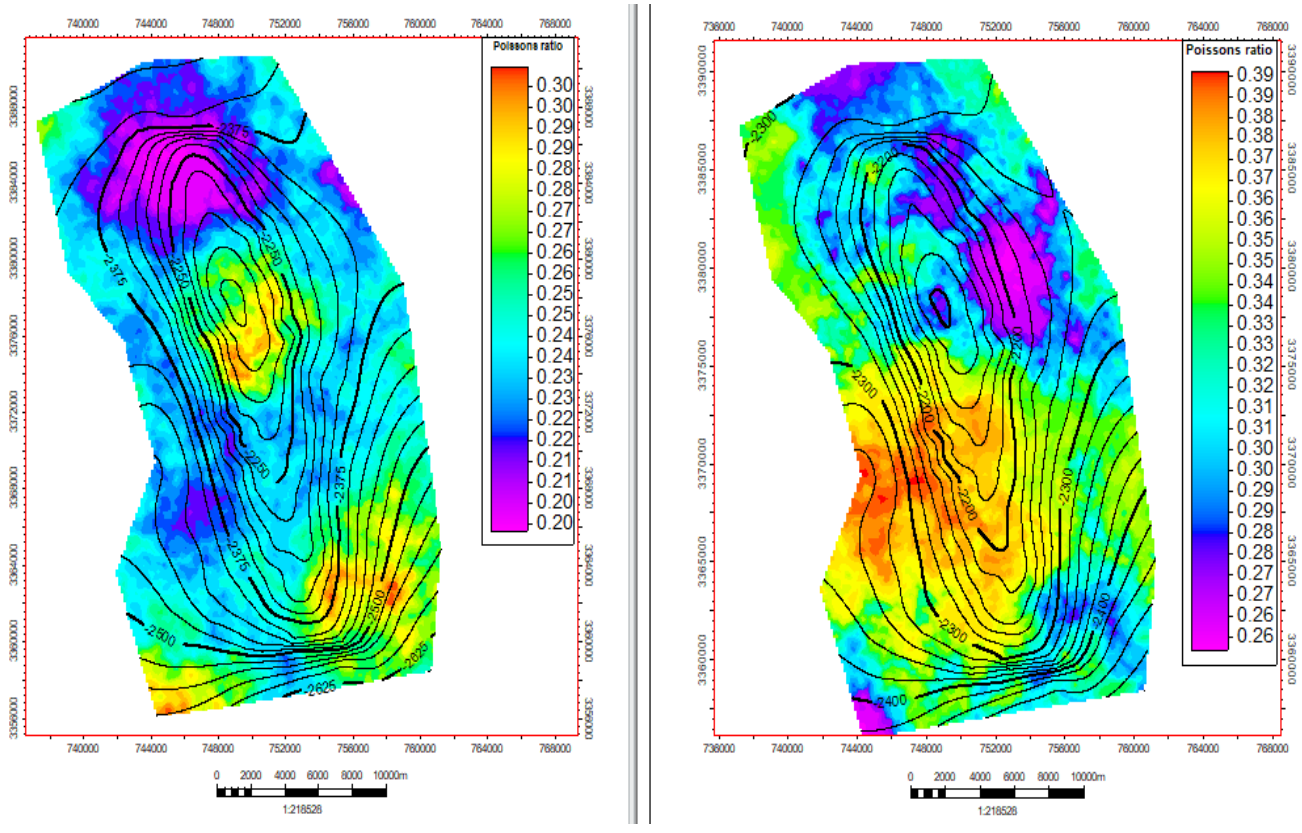

(a) **(b)**

Figure 9: Poisson ratio distribution map for; (a) Mishrif formation and (b) Tanuma formation.

3.2.4 Young's Modulus (E)

Young's modulus was another essential property in mechanical rock properties. The stiff rock that was desired for the wells' stability was referred to by high values of this attribute. The distribution results for Tanuma and Mishrif formations are shown in Figure-10. About 75% of the data in the Tanuma formation was very low, between 0.2 and 0.4 Mpsi, which is mean elastic rock, which is not ideal for well stability. The Mishrif formation had the best and highest values of Young's modulus, indicat ing that it is the most stable.

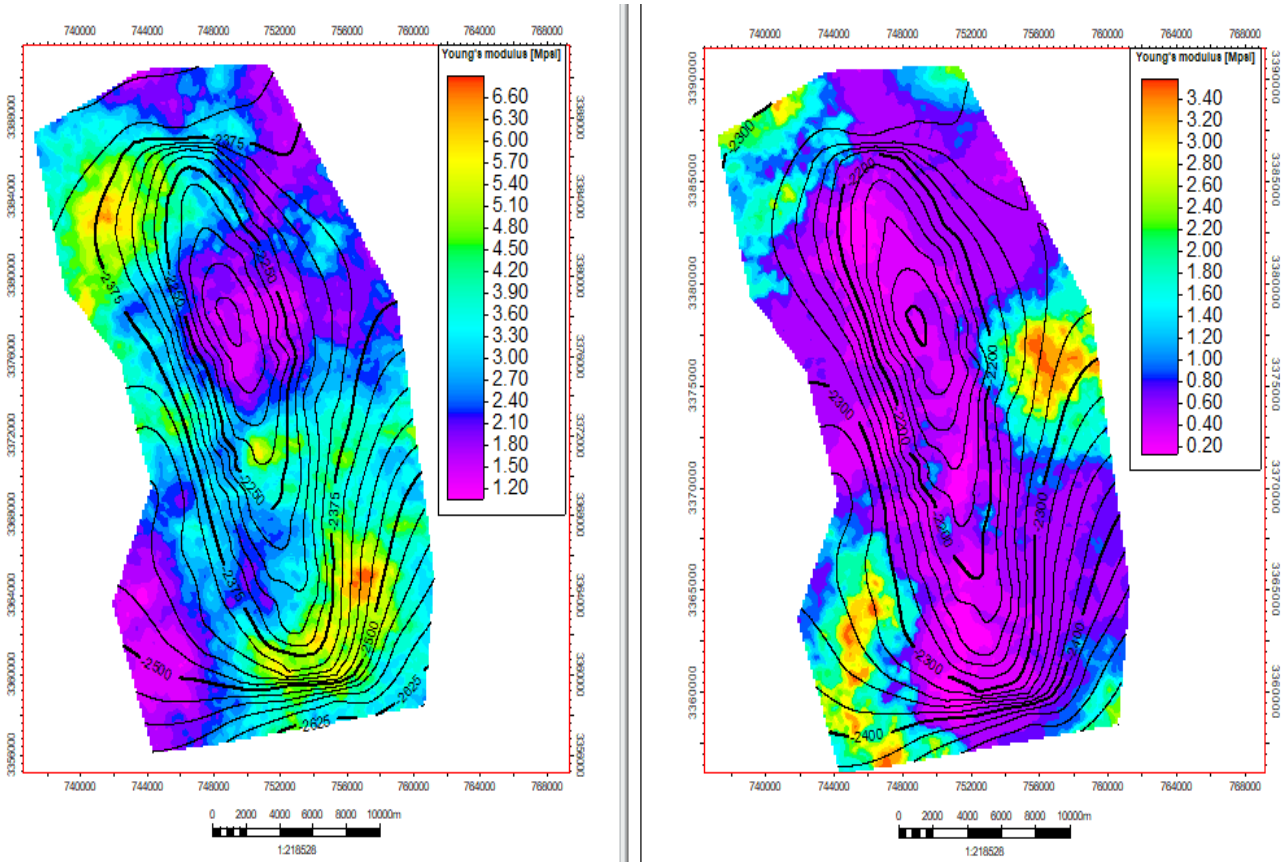

(a) (b)

Figure 10: Young's modulus distribution map for; (a) Mshrif formation and (b) Tanuma formation.

3.2.5 Tensile Strength (TSTR)

The tensile strength is the maximum load that a rock can withstand without cracking [24], and high values of this attribute are desirable for well stability. Figure-11 shows the 3D distribution of the TSTR property, while Figure-12 presents the results of this property for the Tanuma and Mishrif formations. The data indicate that the Tanuma formation is weak and prone to fracture when the tensile strength exceeds 400 psi, as over 75% of the data between 0 and 400 psi were observed in this formation. In contrast, Mishrif exhibited approximately 86% of the data between 600 and 2800 psi, which is excellent. Moreover, the Al-Hammar dome of Mishrif demonstrated 11% of the data between 200 and 600 psi, which is a positive finding.

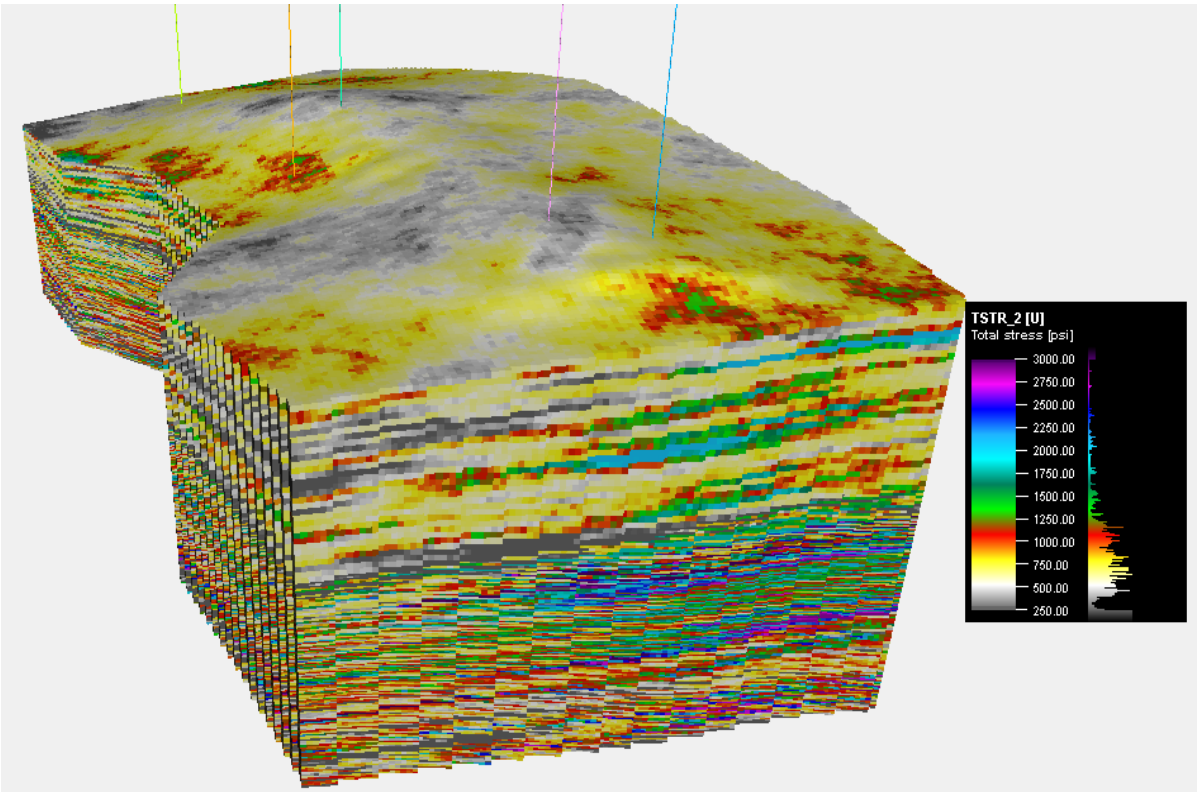

Figure 11: Tensile strength 3D distribution map.

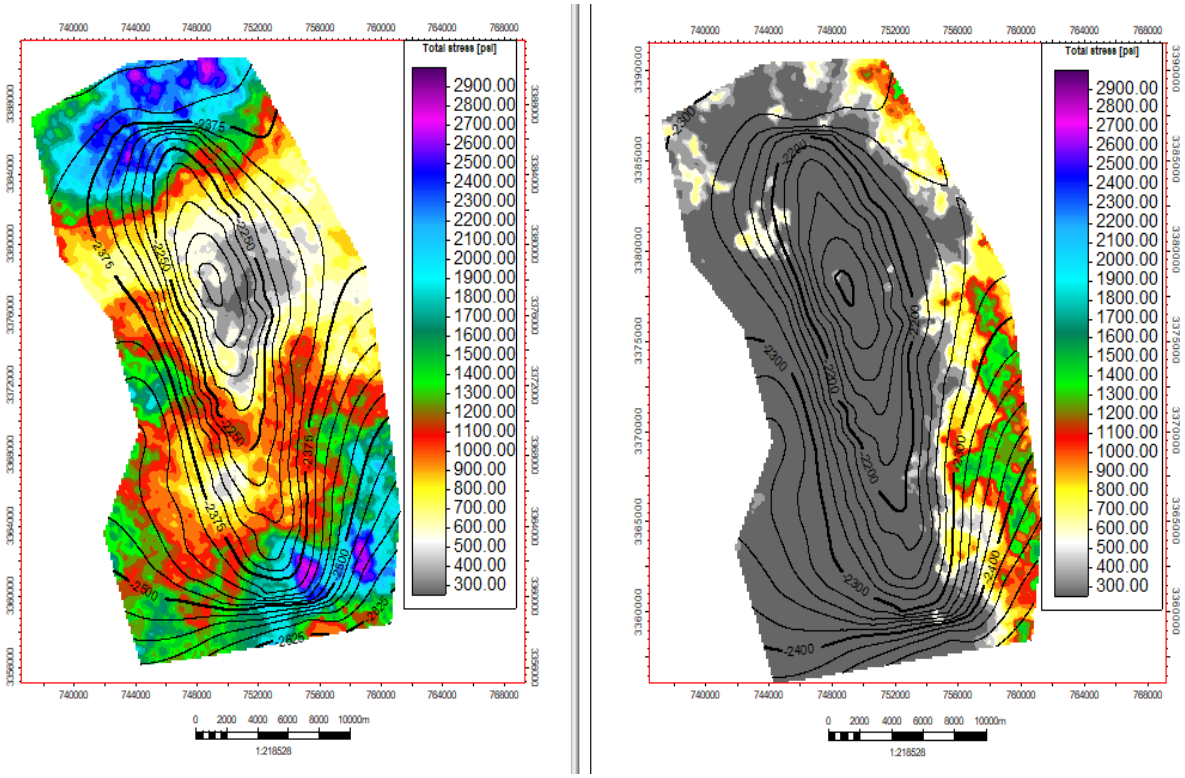

(a) **(b)**

Figure 12: Tensile strength distribution map for; (a) Mishrif formation and (b) Tanuma formation.

3.2.6 Pore Pressure (PP)

One of the basic parameters in the geomechanical model is pore pressure. Pore pressure refers to the pressure of fluid inside the rock area [25]. At shallow depths of 2000 m, pore pressure balances with hydrostatic pressure, but below this depth, overpressure occurs. Pore pressure rises quicker with depth, reaching overburden stress values [26]. The distribution map for Mishrif and Tanuma formations are shown in Figure-13. The highest PP values were found in the Rumilla and Ahmadi formations. To drill safely and economically, the optimal mud weight pressure should be set to control pore pressure.

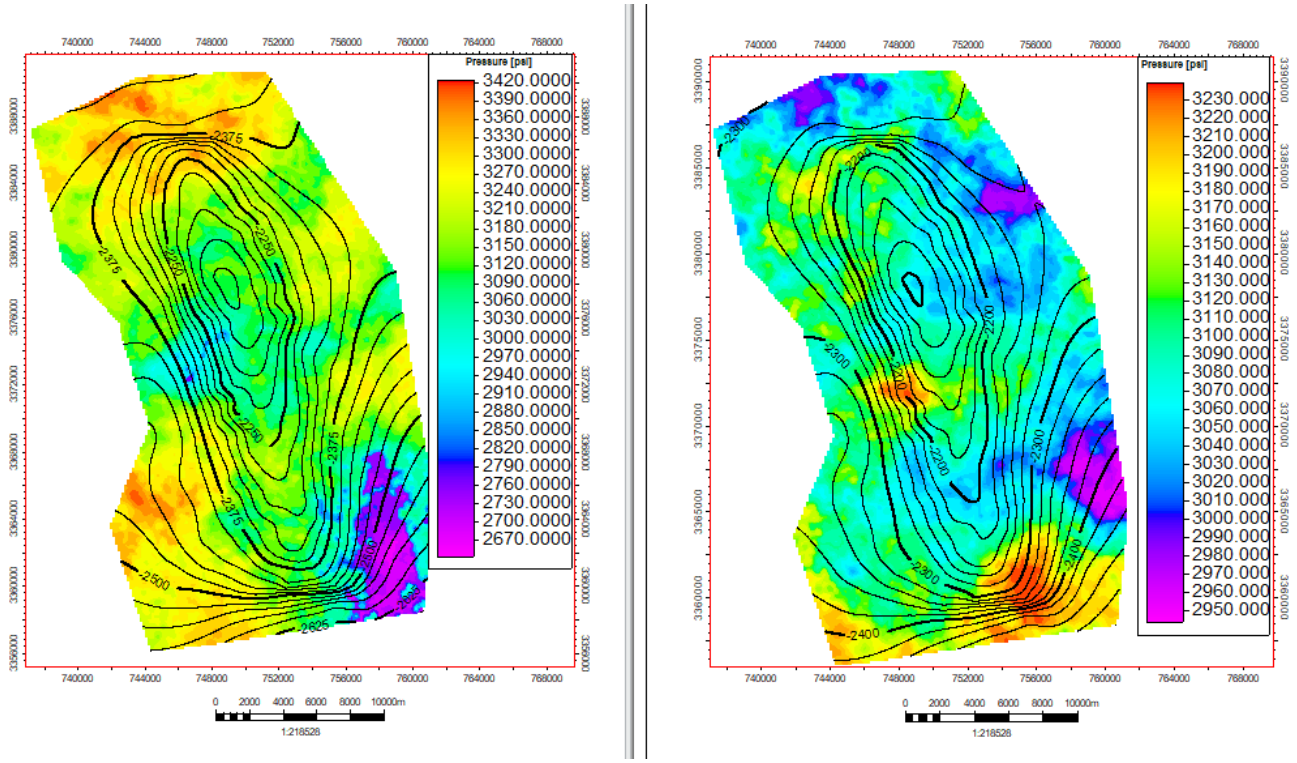

(a) **(b)**

Figure -13 Pore pressure distribution map for; (a) Mishrif formation and (b) Tanuma formation.

3.3. Finite Element Results

In the Zubair oil field, production and injection wells began operating in the Mishrif formation in 2014. For the development and management fields, a 10 years' period was suggested, from 2022 to 2032. The production rate is around 3000 bbl/day, with injection water at 4500 bbl/day. The results reported in Figure.14 below demonstrate that total horizontal stress decreased by about 40 psi in the Shuaiba dome and increased by about 5 psi in the Al-Hammar dome throughout production. The vertical stress still constant during production and injection, indicating compaction and deformation in the reservoir formation. The pore pressure was decreased as a result of the production.

The findings revealed that while the total horizontal stress decreased during depletion, the effective horizontal stress increased slowly due to a reduction in total horizontal stress as formation pressure was depleted. This could result in a rise in differential stress, which could lead to rock shear failure. When the pore pressure increased as a result of the injection, the tensile failure occurred due to a decrease in the differential stress, [27].

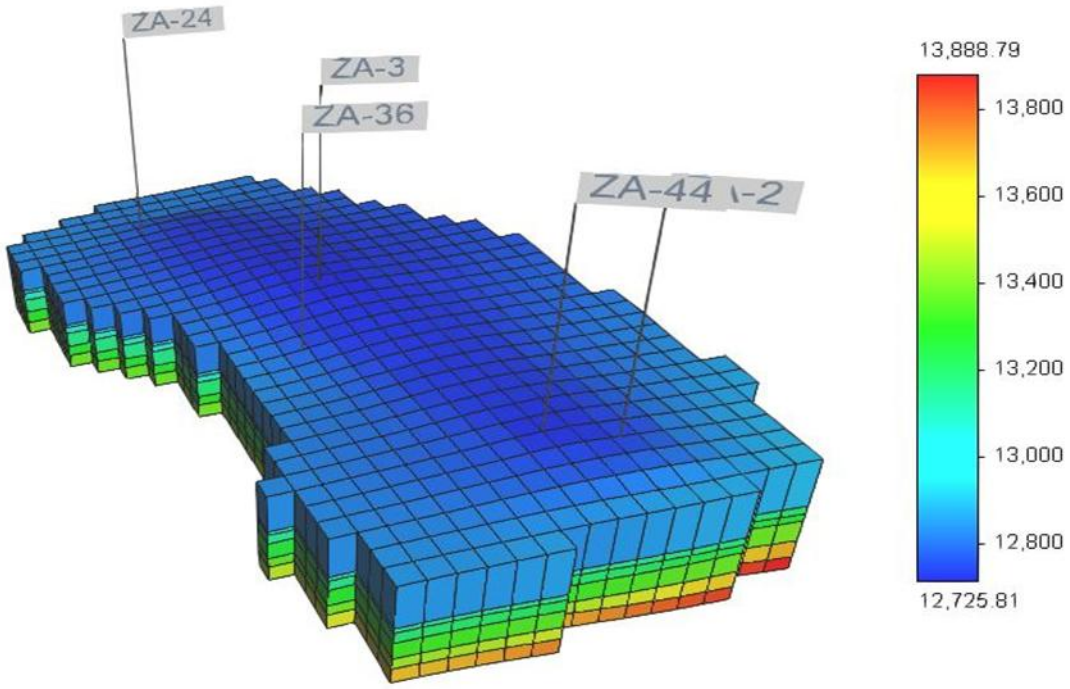

Figure 14: Horizontal stress distribution map after 10 years.

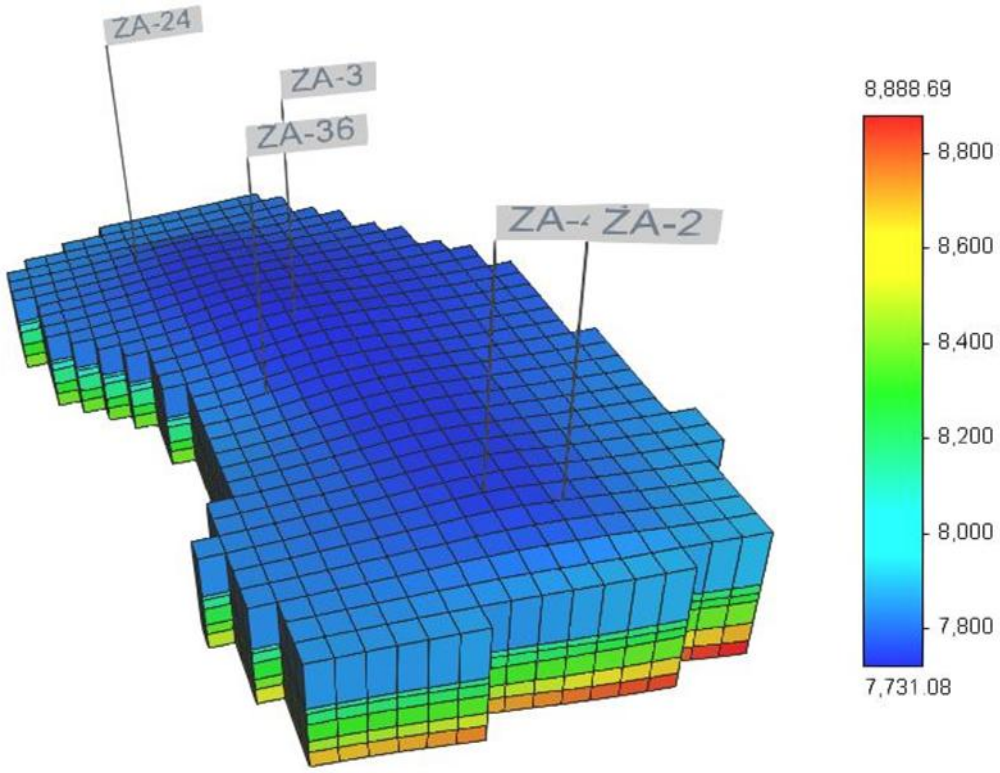

Figure 15: vertical stress distribution map after 10 years.

4. Conclusion

The following conclusions may be made based on the findings from the previous section:

Over the past four decades, the geomechanical model has played a crucial role in the oil industry. Looking ahead, finite element analysis is poised to become the industry's go-to approach. Geomechanical factors, such as rock deformation, fracturing, wellbore stability, compaction, and subsidence, all contribute to the complexity of stress changes during production and injection operations. Typically, reservoir models don't take into account changes in reservoir stresses, which highlights the need for coupling between geomechanical and reservoir models. In a recent 1D study, the calculated horizontal stress enabled us to identify fault regimes, while the calibration data and static mechanical rock properties exhibited a high degree of agreement.

According to the 3D distribution of all mechanical parameters, the Tanuma formation is notably weak, and the weak data are concentrated in the Shuaiba and Al-Hammar domes. The 3D geological model is a useful tool for drilling engineers to determine the optimal location for drilling, with safe mud and a stable wellbore. The 3D distribution shows that the pore pressure is accurately proportional to depth, and there is a depletion in the Mishrif formation, which is a production zone.

A 3D finite element model indicates that as formation pressure depletes, total horizontal stress decreases, causing an increase in effective vertical and horizontal stress, which may trigger rock shear failure. Moreover, injection of water may result in tensile failure due to a decrease in differential stress. Redesigning wells and monitoring changes in rock geomechanics using a 3D finite element model could be a valuable suggestion for future development in the Zubair oil field.

References

[1] J. Whaley, “An Introduction to Geomechanics,” 2019.

[2] R. Rahimi, "The effect of using different rock failure criteria in wellbore stability analysis," Missouri University of Science and Technology, 2014.

[3] M. Zoback, "Reservoir geomechanics," Cambridge university press, 2010.

[4] J.Wan, J. Durlofsky, T. J. R. Hughes, et al., "Stabilized finite element methods for coupled geomechanics-reservoir flow simulations," In SPE Reservoir Simulation Symposium One Petro, 2003.doi: https://doi.org/10.2118/79694-MS.

[5] F.Pan, K. Sepehrnoori, and L.Chin, "Development of a coupled geomechanics model for a parallel compositional reservoir simulator," In SPE Annual Technical Conference and Exhibition. One Petro, 2007.doi: https://doi.org/10.2118/109867-MS.

[6] E. Fjaer, R. M. Holt, P. Horsrud, et al., "Geological aspects of petroleum related rock mechanics," Developments in petroleum science, vol. 53, pp.103-133, 2008.

[7] W. Al-Wardy and O. P.Urdaneta, "Geomechanical modeling for wellbore stability during drilling Nahr Umr shales in a field in petroleum development Oman," In Abu Dhabi International Petroleum Exhibition and Conference. One Petro, 2010 , doi: https://doi.org/10.2118/138214-MS.

[8] M. Mohammad and C.L. Fergusson, "Dextral transpression in Late Cretaceous continental collision, Sanandaj–Sirjan zone, western Iran," Journal of Structural geology, vol. 22, pp. 1125-1139, 2000.

[9] T. Buday and S.Z. Jassim, "The regional geology of Iraq, tectonism, magmatism, and metamorphism," GEOSURV, Baghdad, Iraq,1987.

[10] H. Deng, M. Fu, T.Huang, et al., "Ahdeb oil field, Mesopotamian Basin, Iraq: Reservoir architecture and oil charge history," AAPG Bulletin, vol.102, no. 12, pp.2447-2480, 2018,doi: https://doi.org/10.1306/0424181617217089.

[11] T. K. Al-Ameri, M. S. Jafar and J. Pitman, "Modeling Hydrocarbon Generations of the Basrah Oil Fields," In Southern Iraq, Based on Petromod with Palynofacies Evidence, AAPG Annual Convention and Exhibition, Houston, Texas, pp. 10-13, 2011,doi: https://doi.org/10.3997/2214-4609-pdb.287.1176781.

[12] J.A. Al-Khadhimi, V.K. Sissakian, A.S. Falah, et al., "Tectonic Map of Iraq (Scale 1: 1000000). S.E. of Geological Survey and Mining, Iraq,".1996.

[13] J. Al-Sakini, "Summary of Petroleum Geology of Iraq and the Middle East," Internal Report in Arabic, Northern Petroleum Company, Kirkuk, p.179, 1992.

[14] T.Buday, " The Regional Geology of Iraq Stratigraphy and Palaeogeography," Dar Al-Kutub Publication House, Mosul, vol.1, p.445, 1980.

.

[15] A.K. Faraj, H.A.A. Hussein, and A. N. Abed Al-Hasnawi, "Estimation of Internal Friction Angle for The Third Section in Zubair Oil Field: A Comparison Study," Iraqi Journal of Oil and Gas Research (IJOGR) vol.2, p. 102-111, 2022. doi: http://doi.org/10.55699/ijogr.2022.0202.1031.

[16] B.S. Aadnoy and R. Looyeh, "Petroleum rock mechanics: drilling operations and well design," Gulf Professional Publishing, 2019, doi: https://doi.org/10.1016/C2009-0-64677-8.

[17] A.K. Faraj, and H.A.A. Hussein, "Vertical Stress Prediction for Zubair Oil Field/Case Study," Journal of Engineering, vol. 29, pp.137-152.2023.doi: https://doi.org/10.31026/j.eng.2023.02.09.

[18] G. L. Bowers, "Pore pressure estimation from velocity data: Accounting for overpressure mechanisms besides undercompaction," SPE Drilling & Completion, vol. 10, no. 02, pp. 89-95, 1995, doi: https://doi.org/10.2118/27488-PA.

[19] A.K. Faraj, and H.A.A. Hussein, "Calculation Pore Pressure Utilized Two Methods/Case Study of Zubair Oil Field," Texas Journal of Engineering and Technologyvol. 11, p.1-6, 2022.

[20] Schlumberger, "Techlog Pore Pressure Prediction and Wellbore Stability Analysis Workflow," Solutions Training, 2015.

[21] S. Archer and V. Rasouli, "A log based analysis to estimate mechanical properties and in-situ stresses in a shale gas well in North Perth Basin," Petroleum and Mineral Resources, vol. 21, pp. 122-135, 2012, doi: https://doi.org/10.2495/PMR120151.

[22] A.K. Neeamy, and N.S. Selman, "Building 1D Mechanical Earth Model for Zubair Oilfield in Iraq," Journal of Engineering, vol. 26, no. 5, pp.47-63, 2020, doi: https://doi.org/10.31026/j.eng.2020.05.04.

[23] J. Knappett, "Craig's soil mechanics," London: spon press, vol.8, 2012.

[24] J.C. Jaeger, N.G. Cook, R. Zimmerman, "Handbook of Fundamentals rock mechanics," 4th ed., Black well, New York, 2009.

[25] C. M. Sayers, "An introduction to velocity-based pore-pressure estimation," The Leading Edge, vol. 25, no. 12, pp.1496-1500, 2006, doi: https://doi.org/10.1190/1.2405335.

[26] J.J. Zhang, “Handbook of applied petroleum geomechanics, " Gulf Professional Elsevier, United states, 2019.

[27] R. Hillis, "Pore pressure/stress coupling and its implications for seismicity," Exploration Geophysics, vol. 31, no. 2, pp.448-454, 2000, doi: https://doi.org/10.1071/EG00448.